

Resistive switching characteristics of MnO_x -based ReRAM

Sen Zhang¹, Shibing Long¹, Weihua Guan¹, Qi Liu^{1,2}, Qin Wang¹ and Ming Liu^{1,3}

¹ Laboratory of Nano-Fabrication and Novel Device Integrated Technology, Institute of Microelectronics, Chinese Academy of Sciences, Beijing 100029, People's Republic of China

² College of Electronics and Technology, Anhui University, Hefei 230039, People's Republic of China

E-mail: liuming@ime.ac.cn

Received 7 October 2008, in final form 17 January 2009

Published 19 February 2009

Online at stacks.iop.org/JPhysD/42/055112

Abstract

The resistive switching characteristics of MnO_x thin film were investigated for resistive random access memory (ReRAM) applications. The devices in the form of metal–insulator–metal structure exhibited reversible resistive switching behaviour under both sweeping voltages and voltage pulses. Formation and rupture of conductive filaments were proposed to explain the resistive switching. When Al was used as the top electrode instead of Pt, the device had a better endurance performance. Additionally, the Pt/ MnO_x /Al device showed fast switching speed and long retention ability. The experiment result suggested that Pt/ MnO_x /Al device had a potentiality for practical memory application.

(Some figures in this article are in colour only in the electronic version)

1. Introduction

Based on the resistive change of the insulator in a metal–insulator–metal (MIM) structure, resistance random access memory (ReRAM) possesses the advantages of low power consumption, high operation speed, nondestructive readout, simple structure and good scalability, which is a highly competitive candidate for the generation of nonvolatile memories. A variety of materials have been studied for ReRAM application including ferromagnetic material such as $\text{Pr}_{1-x}\text{Ca}_x\text{MnO}_3$ [1], doped perovskite oxides such as SrZrO_3 [2], organic materials [3] and doped and undoped transition metal oxides (TMOs) [4–11]. Among these materials, TMOs are extensively studied due to their simple structure, easy fabrication process and excellent compatibility with current complementary metal oxide semiconductor (CMOS) technology [4]. Many TMOs have been reported to exhibit resistive switching phenomena, such as NiO [5], ZnO [6], Cu_2O [7], ZrO_2 [8, 9], TiO_2 [10] and Nb_2O_5 [11]. It is thought that resistive switching is an intrinsic property of TMOs, and all doped and undoped TMOs can exhibit resistive switching [12]. However this hypothesis needs to be confirmed since many other TMOs have not been studied.

In this paper, we investigate the resistive switching behaviour of manganese oxides, which have rarely been reported before. The manganese oxide film was deposited by electron beam evaporation and sandwiched between two metal electrodes in the forms of Pt/ MnO_x /Pt and Pt/ MnO_x /Al. These devices exhibited stable resistive switching behaviour under dc sweeping voltages. It was noticed that Pt/ MnO_x /Al device had a better endurance performance than Pt/ MnO_x /Pt, which could be due to aluminium depriving oxygen from the MnO_x thin film. The study of MnO_x may help to achieve a better understanding of resistive switching characteristics of TMOs.

2. Experimental details

The MnO_x -based memory devices were fabricated as follows: (100)-oriented silicon wafers were chemically cleaned, and then a 150 nm thick SiO_2 film was thermally grown. A Ti layer and Pt film (with thicknesses of 10 nm and 50 nm, respectively) were deposited sequentially onto the substrates by electron beam evaporation. Ti was used as an adhesive layer and Pt served as the bottom electrodes (BEs). After that, a 150 nm thick MnO_x thin film was e-beam evaporated onto the Pt film using a MnO_2 target in an ambient pressure of 2.6×10^{-6} Torr at room temperature (RT). Finally

³ Author to whom any correspondence should be addressed.

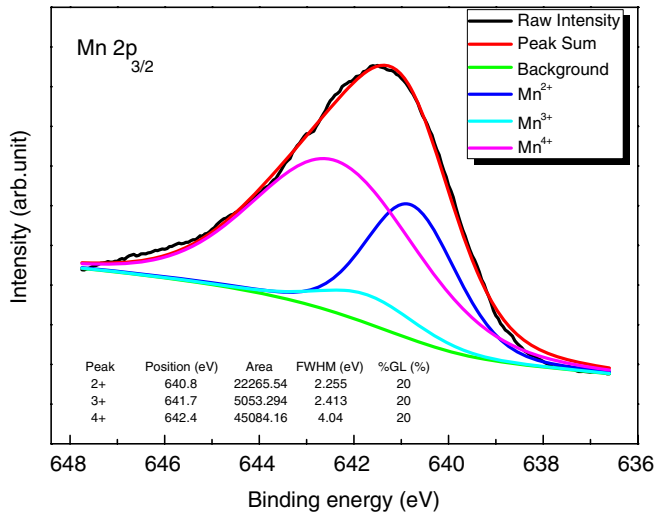


Figure 1. XPS spectra of Mn $2p_{3/2}$ of the as-deposited MnO_x film. The film was deposited by e-beam evaporation using MnO_2 target in a vacuum condition. In the evaporation, MnO_2 would decompose so that the manganese element was at different chemical states.

50 nm thick square-shaped Al or Pt top electrodes (TEs) with dimensions ranging from $50 \times 50 \mu\text{m}^2$ to $800 \times 800 \mu\text{m}^2$ were deposited and defined by photolithography and lift-off process. X-ray photoelectron spectroscopy (XPS) analysis was utilized to investigate the chemical states of the MnO_x matrix. The current–voltage characteristics of the fabricated devices were measured by a Keithley 4200-SCS semiconductor characterization system. The pulse test was performed with an Agilent 81110A Pulse Pattern Generator and a Tektronix DPO7104 digital phosphor oscilloscope.

3. Results and discussion

X-ray photoelectron spectroscopy (XPS) was employed to investigate the chemical states of the deposited films. The raw Mn $2p_{3/2}$ peak was at 641.5 eV. The best fitted spectral result is shown in figure 1. The ‘Shirley + Linear’ background was used, and the spectral lines were Gaussian–Lorentzian. The three peaks were attributed to the existence of Mn^{4+} (642.4 eV), Mn^{3+} (641.7 eV) and Mn^{2+} (640.8 eV), respectively [13]⁴. The MnO_x film was deposited by electron beam evaporation using the MnO_2 target. It was well known that MnO_2 would decompose on heating to form lower oxides [14]. Hence, the deposited film was very likely to consist of different manganese oxides. According to the XPS result, most of the manganese element existed in the form of MnO and MnO_2 . Such mixed oxides were naturally imperfect in the microstructure, and metallic ions or oxygen vacancies were very likely to exist in the matrix. Those defects were thought to play important roles in resistance hysteresis [5, 8–10].

Figure 2 shows the typical I – V curves of both Pt/ MnO_x /Pt and Pt/ MnO_x /Al devices. The inset of figure 2 is the schematic

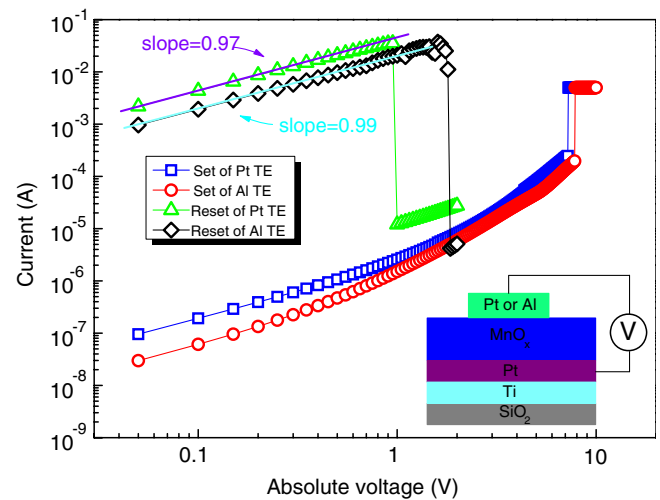


Figure 2. Double logarithmic plots of I – V curves of Pt/ MnO_x /Pt and Pt/ MnO_x /Al devices. The inset is the schematic plot of electrical measurement configuration. Switching between HRS and LRS could be achieved by voltages of arbitrary polarity. The slopes of LRS curves are close to one, indicating Ohmic conduction.

configuration of the measurement. Sweeping voltages were applied to the TEs of the sandwich devices while Pt BEs were grounded. The pristine devices were in the high resistance state (HRS). When the voltage went from zero to a high voltage, an abrupt current increase occurred at about 8 V, indicating the devices changed to a low resistance state (LRS). This soft breakdown is the so-called ‘set’ process, corresponding to the ‘writing 1’ process of memories. The current flowing through the devices was limited to a maximum value by the test equipment to protect the devices from perpetual breakdown. After set on, a sweeping voltage without current compliance was applied again, and a dramatic current drop appeared, indicating that the devices changed back to the HRS, which is the so-called ‘reset’ process. The switching between high and low resistance could be done repeatedly. Set and reset operations could be achieved under positive and negative voltages, and they could be done in succession changing or unchanging voltage polarity. That is, the resistance switching did not depend on the polarity of the applied voltage and it was defined as nonpolar resistive switching characteristic [15]. Resistance switching under voltage pulses was also feasible. Set operation could be induced by a 100 ns pulse of 12 V and reset by a 200 ns pulse of 2 V.

Several hypothetical models have been proposed to explain resistive switching phenomena, such as formation and rupture of conductive filaments [10], trap charging and discharging [9] and modulation of Schottky barrier height [16, 17]. But until now, the underlying mechanism is still controversial. On the basis of the measured electrical characteristics, the filamentary mechanism is appropriate to explain our devices resistance switching. According to the filamentary mechanism, when the electric field is high enough, defects such as oxygen vacancies or metallic ions align to form conductive filaments which connect the two electrodes. After the conductive filaments are formed, the current flows mainly

⁴ A small calibration was made to the data. In XPS analysis C 1s was used as a standard for the correction of charging effects. The authors of [13] took the energy of C 1s as 285.0 eV, now it was more reliably determined to be 284.8 eV. So there was a shift of 0.2 eV.

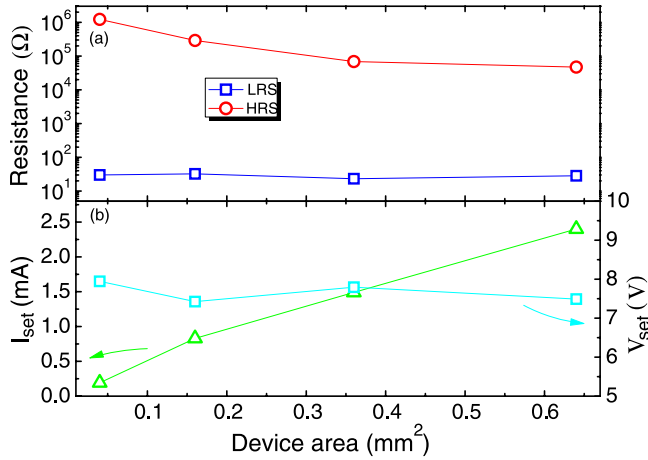


Figure 3. (a) The relationship of high and low resistances of Pt/MnO_x/Al devices to the device sizes; (b) the dependences of set current and set threshold voltage of Pt/MnO_x/Al on the device sizes.

through the filaments and the devices turn to low resistance and exhibit Ohmic behaviour, which is consistent with the unity slope of the double-logarithmic-plotted LRS I – V curves in figure 2. During the reset process, these conductive filaments break off as a result of the Joule heating generated by large current, which makes the devices turn back to the HRS.

It was found that the endurance property of Pt/MnO_x/Al was much better than that of the Pt/MnO_x/Pt device. Most of the Pt/MnO_x/Pt devices broke down after a few set/reset cycles, and then acted as stable low value resistors, while several Pt/MnO_x/Al devices could still function after more than 100 dc switching cycles under the condition that the devices were set by negative sweeping voltages. It is proposed that more oxygen vacancies caused by aluminium depriving oxygen from the MnO_x layer are the reason for the endurance difference. Aluminium is known to be able to get oxygen from TMOs to form oxides [18]. According to the filamentary mechanism, during the set process, conductive filaments propagate from the cathode and filaments at the anode side are weaker (or less conductive) than the ones near the cathode. The filaments rupture in a localized region near the anode during the reset process and recover in the subsequent set process [10]. The rest of the filaments are preserved during the whole switching process. As to our situation, the filaments broke and recovered in the MnO_x layer⁵. This layer had been deprived of oxygen by the aluminium electrode and possessed more oxygen vacancies, making conductive filaments' formation or recovery easier, so the Pt/MnO_x/Al devices exhibited an improved endurance property.

Figure 3(a) depicts the dependences of high and low resistance of the Pt/MnO_x/Al devices on the size of the TEs.

⁵ Although aluminium oxide thin films have been found to exhibit resistive switching behaviour [19], the switching of the Al/MnO_x/Pt device should be dominated by the bulk of MnO_x, because Pt/MnO_x/Al and Pt/MnO_x/Pt have almost the same I – V behaviour. As to the stacked structures of Al₂O₃/TiO₂ and Al₂O₃/TiO₂/Al₂O₃, the switching properties were mostly governed by the farthest layers from the cathode since the conductive filaments in the films near the cathode were unchanged [20].

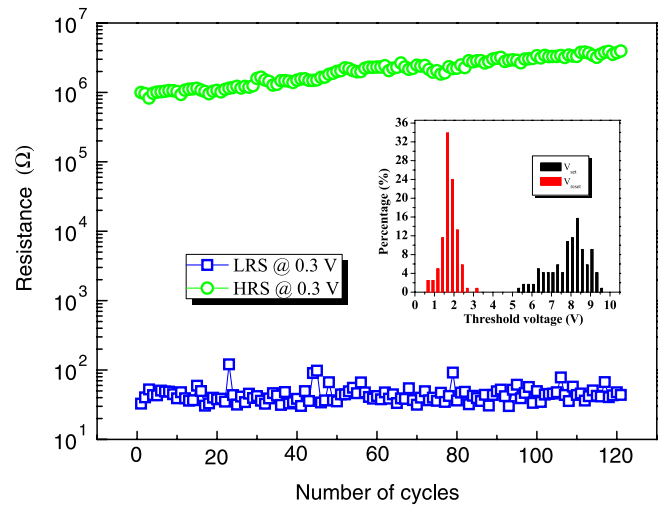


Figure 4. Resistance values versus cycle numbers for a $200 \times 200 \mu\text{m}^2$ Pt/MnO_x/Al device. The inset is the distribution of threshold voltages.

With the increase in the size of the TEs, the resistances of the HRS of the Pt/MnO_x/Al device got smaller, while the values of the LRS showed no dependence on the device sizes, which was in agreement with the localized conductive filament mechanism. As shown in figure 3(b), V_{set} (defined as the threshold voltage where set switching occurred) had little reliance on the cell area, while I_{set} (defined as the current when the set occurred) increased with larger cell size. This indicates that the electrical field required to form conductive filaments is constant and the conduction of the HRS is almost homogeneous. Those properties suggest that Pt/MnO_x/Al devices have considerable advantages in regard to scalability.

Shown in figure 4 is the dependence of the resistance on the repetitive switching cycles of a $200 \times 200 \mu\text{m}^2$ Pt/MnO_x/Al device. The device was set by negative voltage and reset by positive voltage. Resistance values were obtained at 0.3 V. As can be seen from the experimental data, the low resistance values were distributed in a narrow range around 100Ω , while the high resistance values were around $1 \text{ M}\Omega$. The narrow dispersion of resistance values guarantees a sensing margin larger than three orders. Uniformity of memory parameters such as resistance values is very important for practical application. Compared with some other TMO based devices [6, 7, 11], the Pt/MnO_x/Al memory devices exhibited better uniformity of resistances. The inset of figure 4 depicts the distribution of the threshold voltages for set and reset (V_{set} and V_{reset}). There is no overlap between V_{set} and V_{reset} , which ensures the MnO_x-based device can be well operated in the application of ReRAM. To further confirm the potentiality of practice memory application, the state retention property of Pt/MnO_x/Al was checked at RT and 85°C , respectively. Figure 5 shows the time-dependent resistance evolution. The test at RT was done for over 10^5 s and retention at 85°C was over 10^4 s. In both situations, the resistances of LRS exhibited little change, while those of HRS became larger, resulting

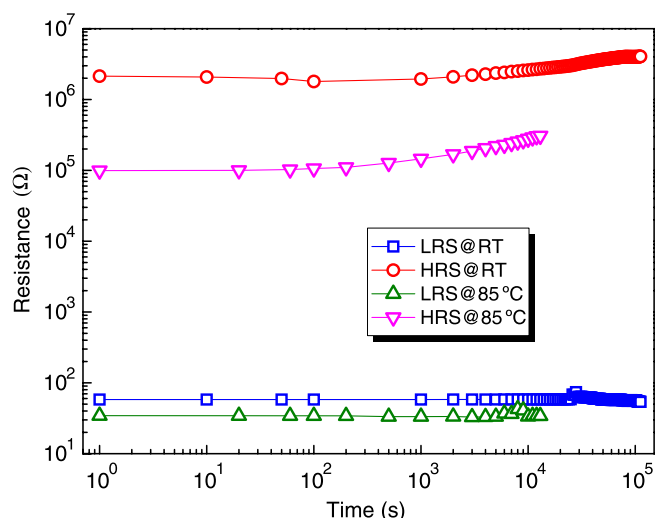


Figure 5. Retention performance of the Pt/MnO_x/Al device at RT and 85 °C. The gap between the two HRS was due to the conductivity difference induced by temperature.

in larger HRS/LRS ratios, and enhanced the memory's reliability.

4. Conclusions

In summary, the resistive switching characteristics of MnO_x-based ReRAM were investigated for nonvolatile resistance memory applications. It was found that devices of both Pt/MnO_x/Pt and Pt/MnO_x/Al exhibited the reversible nonpolar resistance switching phenomenon. The switching between HRS and the LRS could be achieved under dc sweeping voltage as well as pulse voltages. According to the electrical characteristics, we proposed that the resistance switching was caused by the formation and rupture of conductive filaments. The Pt/MnO_x/Al devices exhibited better endurance performance than the Pt/MnO_x/Pt devices. The resistance evolution with cycles and the nonvolatile property of the Pt/MnO_x/Al structure were also demonstrated. The ratio of high resistance to low resistance was over three orders of magnitude and the resistance values of both states showed narrow dispersions in 100 cycles. Time-dependent tests showed the devices had good retention properties. All the experimental data suggested that the Pt/MnO_x/Al device had the potential for future memory application.

Acknowledgments

This work was supported by the Hi-Tech Research and Development Program of China (863 Program) under Grant Nos 2008AA031403 and 2008AA031401, the National Basic Research Program of China (973 Program) under Grant Nos 2006CB302706, 2006CB806204 and 2007CB935302, the National Natural Science Foundation of China under Grant Nos 60825403, 90607022 and 60506005, and the Chinese Academy of Sciences under Grant No YZ200840.

References

- [1] Liu S Q, Wu N J and Ignatiev A 2000 *Appl. Phys. Lett.* **76** 2749
- [2] Beck A, Bednorz J G, Gerber C, Rossel C and Widmer D 2000 *Appl. Phys. Lett.* **77** 139
- [3] Jung J H, Kim J H, Kim T W, Song M S, Kim Y H and Jin S 2006 *Appl. Phys. Lett.* **89** 122110
- [4] Baek I G et al 2004 *Electron Devices Meeting, IEDM Tech. Dig.* pp 587–90
- [5] Seo S et al 2005 *Appl. Phys. Lett.* **85** 5655
- [6] Chang W Y, Lai Y C, Wu T B, Wang S F, Chen F and Tsai M J 2008 *Appl. Phys. Lett.* **92** 022110
- [7] Chen A et al 2005 *Electron Devices Meeting IEDM Tech. Dig.* pp 746–9
- [8] Lee D, Choi H, Sim H, Choi D, Hwang H, Lee M J, Seo S A and Yoo I K 2005 *IEEE Electron Device Lett.* **26** 719
- [9] Liu Q, Guan W H, Long S B, Jia R, Liu M and Chen J N 2008 *Appl. Phys. Lett.* **92** 012117
- [10] Kim K M, Choi B J, Shin Y C, Choi S and Hwang C S 2007 *Appl. Phys. Lett.* **91** 012907
- [11] Sim H, Choi D, Lee D, Seo S, Lee M J, Yoo I K and Hwang Y 2005 *IEEE Electron Device Lett.* **26** 292
- [12] Hsu S T and Li T K 2007 *RRAM electronics and switching mechanism Mater. Res. Soc. Symp. Proc.* **997**
- [13] DiCastro V and Polzonetti G 1989 *J. Electron Spectrosc. Relat. Phenom.* **48** 117
- [14] Dakhel A A 2006 *Thin Solid Films* **496** 353
- [15] Inoue I H, Yasuda S, Akinaga H and Takagi H 2008 *Phys. Rev. B* **77** 035105
- [16] Sim H, Choi H, Lee D, Chang M, Choi D, Son Y, Lee E H, Kim W, Park Y D, Yoo In-K and Hwang H 2005 *Electron Devices Meeting, IEDM Tech. Dig.* pp 758–61
- [17] Sawa A, Fujii T, Kawasaki M and Tokura Y 2004 *Appl. Phys. Lett.* **85** 4073
- [18] Wu X, Zhou P, Li J, Chen L Y, Lu H B, Lin Y Y and Tang T A 2007 *Appl. Phys. Lett.* **90** 183507
- [19] Kim S and Choi Y K 2008 *Appl. Phys. Lett.* **92** 223508
- [20] Kim K M, Choi B J, Koo B W, Choi S, Jeong D S and Hwang C S 2006 *Electrochem. Solid-State Lett.* **9** G343